### III. Experimental Results

The method has been implemented in Fortran and it was tested using real ECG's from our own ECG library and from the standard CSE ECG library [3]. It is noted that these two libraries contain rest ECG's.

For illustrative purposes some cardiac cycles from various ECG's are given in Fig. 3 together with the results of the recognition of the *ST* segment. The calculated onsets and endpoints of the *ST* segments are marked with up-arrows.

It was observed that the $L_\infty$ error norm gives results for the onset and the endpoint of the *ST* segment which are close to the ones found by visual recognition. For this reason, this error norm is recommended in conjunction with the method presented for the recognition of the *ST* segment.

It is noted that the results the method gives for the various *ST* segments, recorded from the same subject, are the same provided that the noise content is about the same in all *ST* segments. This implies that filtering should be performed prior to *ST* segment recognition by this method.

### IV. Concluding Remarks

The method presented in this paper has not been gone through a strict evaluation procedure because of lack of a test set of data. Despite it, it can be said that the results taken so far are satisfactory and so the method deserves consideration.

### References

[1] J. S. Weisner, W. J. Tompkins, and B. M. Tompkins, "A compact, microprocessor based ECG *ST*-segment analyzer for the operating room," *IEEE Trans. Biomed. Eng.*, vol. BME-29, pp. 624–648, Sept. 1983

[2] D. Pavlidis, "Waveform segmentation through functional approximation," *IEEE Trans. Comput.*, vol. C-22, pp. 689–697, July 1973.

[3] J. L. Willems *et al.*, "Establishment of a reference library for evaluating computer ECG measurement programs," *Comput. Biomed. Res.*, vol. 18, pp. 439–457, 1985.

## Analysis of Models for External Stimulation of Axons

FRANK RATTAY

***Abstract*—Extracellular electrodes produce electrical fields at the outside of nerve fibers. Discretization of the axon's length coordinate allows simulation of the excitation by a system of differential equations in time, and difference equations in space. For myelinated fibers this segmentation is naturally given by the nodes of Ranvier, whereas unmyelinated axons can be segmented arbitrarily. In both cases the equations are similar and can be treated in parallel. The activity of the axon depends on the second space derivative of the extracellular medium. The activating function is discussed for monopolar electrodes but the principle can be extended to arbitrary configurations of electrodes.**

### Introduction

Many papers are concerned with the quantitative description of intracellular and extracellular fields, e.g., [1]–[3], but with the exception of McNeal's model [4] there is no efficient model in use to compute the reaction of an axon which is stimulated by extracellular electrodes. Starting with his model for subthreshold stimulation of unmyelinated fibers, we will develop a method also valid for superthreshold stimulation. This model applies for unmyelinated as well as for myelinated fibers and most differences in the results are only of quantitative nature.

Manuscript received May 28, 1985; revised May 19, 1986.

The author is with the Institut für Analysis , Technische Mathematik und Versicherungmathematik, Technical University of Vienna, A-1040 Vienna, Austria.

IEEE Log Number 8609986.

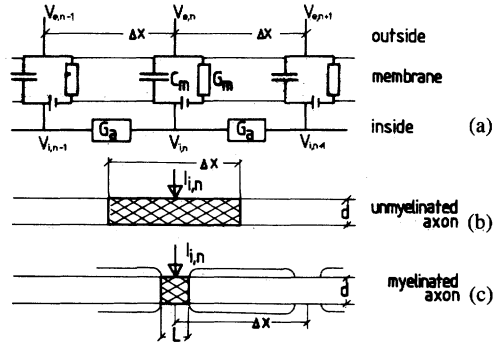


Fig. 1. (a) Segmentation of an axon allows us to study the excitation process by an analogous electrical network. (b) The active part of one segment of membrane for the unmyelinated and (c) the myelinated case cross hatched. In (b) the segmentation length $\Delta x$ has to be chosen so small that computational errors are low, whereas in (c) $\Delta x$ is equal to the distance of the node of Ranvier.

The membrane of the nerve fiber is approximated by an electric network consisting of voltage source, capacity, and resistance as shown in Fig. 1(a). In the case of unmyelinated fibers, the computation uses segments labeled $n = 1, 2, \ldots$ of length $\Delta x$ within which all points of the membrane have the same properties [Fig. 1(b)]. In myelinated fibers active parts exist only at the nodes of Ranvier of width $L$ which are spaced by $\Delta x$ along the membrane [Fig. 1(c)]. The ionic current $I_i$ passing through the $n$th active part of the membrane with capacity $C_m$ is denoted by $I_{i,n}$. $I_{i,n}$ is a function of the voltage between the inside potential $V_{i,n}$ and the outside potential $V_{e,n}$. The current running in the axon is driven through the axon conductance $G_a$ by the inside potentials at the locations $n-1$, $n$, and $n+1$. At the part $n$ of the membrane, according to Fig. 1, the following equation for the currents results.

$$C_m \cdot d(V_{i,n} - V_{e,n})/dt + I_{i,n} + G_a(V_{i,n} - V_{i,n-1}) + G_a(V_{i,n} - V_{i,n+1}) = 0. \quad (1)$$

Setting $V_r$ equal to the inner resting potential, the reduced voltages

$$V_n = V_{i,n} - V_{e,n} + V_r \quad (2)$$

are defined and $V_n$ substituted into (1) gives

$$dV_n/dt = (G_a \cdot (V_{n-1} - 2V_n + V_{n+1} + V_{e,n-1} - 2V_{e,n} + V_{e,n+1}) - I_{i,n})/C_m. \quad (3)$$

The ionic current $I_{i,n}$ is a function of $V_n$ and $t$ and can be modeled by the four well known Hodgkin–Huxley differential equations (HH) [5], [6] for the unmyelinated axon. Frankenhaeuser and Huxley found five other differential equations (FH) to describe $I_{i,n}$ in the myelinated fiber [7], [4]. The HH and FH equations are nonlinear and difficult to analyze. For some problems it is more appropriate to use simpler models for $I_{i,n}$ [6].

Equation (3) shows the influence of the external potentials $V_{e,n}$, which are generated by the stimulating external electrodes positioned at some distance from the axon, on the inner distribution $V_n$. Equation (3) is basic for the determination of the threshold currents of electrodes for a given geometry. $V_{e,n}$ is determined by the electrode positions and the conductivity of the outside medium.

### The Unmyelinated Axon

Although the classical Hodgkin–Huxley experiments were carried out on the giant squid axon, differences in external potentials caused by the thickness of the axon are neglected in the following considerations. McNeal has given some attention to this simplification [4].

The ionic current $I_i = i_{Na} + i_K + i_L$ consists of sodium, potassium, and leakage current given by the further HH equations. With $r_s - a$ resistance/cm and $G_a = 1/r_s \Delta x$, (3) becomes

$$\frac{dV_n}{dt}\left[\frac{\text{mV}}{\text{ms}}\right] = \frac{1}{C_m[\mu\text{F}]} \cdot \left\{ \frac{1}{r_s\,[\text{k}\Omega/\text{cm}] \cdot \Delta x[\text{cm}]} \cdot (V_{n-1} - 2V_n + V_{n+1} + V_{e,n-1} - 2V_{e,n} + V_{e,n+1})\,[\text{mV}] - \pi d \Delta x[\text{cm}^2] \cdot (i_{Na} + i_K + i_L)_n[\mu\text{A/cm}^2] \right\} \quad (4)$$

with $r_s = 4\rho_i/\pi d^2$, $\rho_i$ being the resistivity of axoplasm, and $d$ being axon diameter. Introducing $c_m$ as the capacitance per cm$^2$ and

$$C_m = \pi \cdot d \cdot \Delta x \cdot c_m \quad (5)$$

leads to

$$\frac{dV_n}{dt} = \frac{1}{c_m} \cdot \left\{ \frac{1}{r_s d \pi} \left( \frac{V_{n-1} - 2V_n + V_{n+1}}{\Delta x^2} + \frac{V_{e,n-1} - 2V_{e,n} + V_{e,n+1}}{\Delta x^2} \right) - (i_{Na} + i_K + i_L)_n \right\}. \quad (6)$$

Equation (6) is the version of (3) for the unmyelinated axon and allows the simulation of the fiber in the time dependent electrical field. For electrical stimulation, it is important to recognize that the second derivative of the external potential in the direction of the axon is responsible for all the activations inside the axon. With

$$\bar{S}(x, t) = (V_{e,n-1} - 2V_{e,n} + V_{e,n+1})/\Delta x^2 \quad (7)$$

taking the limit for $\Delta x \to 0$, we find the activating function $S$

$$\bar{S} \to S = \partial^2 V_e / \partial x^2 \quad (8)$$

and writing $\bar{r}_s = r_s d \pi$ we get from (6) a version of the partial HH equation to simulate extracellular stimulation of axons.

$$\partial V/\partial t = \frac{1}{c_m}\left( \frac{1}{\bar{r}_s} + \partial^2 V/\partial x^2 - I_i(V, t) + \frac{S(x, t)}{\bar{r}_s} \right). \quad (9)$$

It is convenient to define a sum of current densities

$$I = \frac{1}{\bar{r}_s}(\partial^2 V/\partial x^2 + S). \quad (10)$$

In the case of the HH voltage clamped experiments $\partial^2 V/\partial x^2 = 0$ and (9) is reduced to the ordinary HH equation

$$\dot{V} = \frac{1}{c_m}(I - I_i) \quad (11)$$

where $I$ is the current injected per cm$^2$. The ionic current is

$$I_i = i_{Na} + i_K + i_L = g_{Na} m^3 h (V - V_{Na}) + g_K n^4 (V - V_K) + g_L (V - V_L) \quad (12)$$

where $g_{Na}$, $d_K$, and $g_L$ are conductances and $V_{Na}$, $V_K$, $V_L$ are equilibrium potentials. The probabilities $m$, $n$, $h$ are explicitly given by the ordinary HH equation [5] which have been extensively studied [6], [8]–[10]. The threshold of the stimulating current $I_{th}$ depends on pulse shape and duration. The strength duration curve (Fig. 2) shows the threshold current density $I_{th}$ for square impulses of duration $T$ which has to be reached according to (11) to produce an action potential but it can be used only for very rough estimations of electric currents because the influence of spatial propagation is neglected. Equation (11) applies to intracellular injection of current. The merit of (6) resp. (9) is that it allows the determination of current which flows in an external stimulating electrode accessible for measurement.

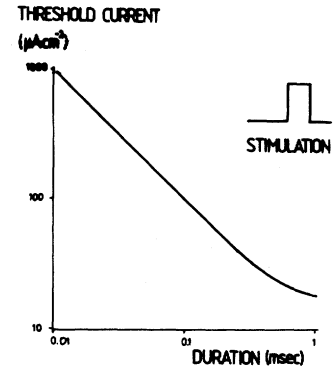


Fig. 2. Strength duration curve calculated with the ordinary Hodgkin–Huxley equations for standard squid data, but with $T = 29°C$. Ordinate measures current density at the membrane. Current injection is intracellular.

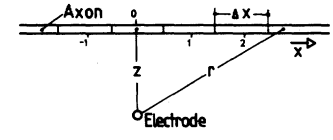


Fig. 3. A monopolar electrode at distance $z$ produces symmetric effects at positions $x$ and $-x$. Segments of length $\Delta x$ are those of a network according to Fig. 1(a).

As an example, the excitation by a monopolar spherical electrode which is imbedded in a homogeneous extracellular medium with resistivity $\rho_e$ will be considered. The electrode has a distance $z$ from the axon according to Fig. 3. We assume spherical symmetry around the tip of the electrode. The electrical potential $V_e$ at the distance $r$ from the electrode under these simple assumptions is

$$V_e = \rho_e \cdot I_{el}/4\pi r \quad (13)$$

where the current $I_{el}$ flows from the electrode. This arrangement is symmetric and measuring $x$ from the point 0 (Fig. 3), (13) becomes

$$V_e = \frac{\rho_e}{4\pi} \cdot (z^2 + x^2)^{-1/2} \cdot I_{el}(t) \quad (14)$$

and the activating function

$$d^2 V_e/dx^2 = g(x, z) \cdot I_{el}(t) = \frac{\rho_e}{4\pi} \cdot (z^2 + x^2)^{-5/2} \cdot (2x^2 - z^2) \cdot I_{el}(t) \quad (15)$$

is the product of a space function and a time function. $V_e$ and $\partial^2 V_e/\partial x^2$ are shown as the full lines (Fig. 4) for a constant electrode current coming from a cathodal electrode with $z = 1$ mm.

Starting from rest at $V = 0$, $\partial V/\partial t$ has to be positive in order to approach the threshold voltage at the most excitable location 0. Therefore, according to (9), $d^2 V_e/dx^2$ has to be positive and from (15) for $x = 0$, $I_{el}$ has to be cathodal. It is seen from (15) that $I_{el} < 0$ allows excitation of the axon only for

$$|x| < z/\sqrt{2}. \quad (16)$$

We note that this follows from purely geometric considerations.

The potential $V_e(x)$ (14) and the second derivative $d^2 V_e/dx^2$ (15), which we call the activating function as it is responsible for the excitation, is shown in Fig. 4 for the cathodal threshold current $I_{\bar{el},th}$. It is seen from the figure that $\partial^2 V_e/\partial x^2$ decreases quickly and parts more distant than $5z$ (=5 mm) are not activated; therefore, they need not be considered in a simulation not concerned with propagation although $V_e$ does not vanish there. As illustrated [Fig.

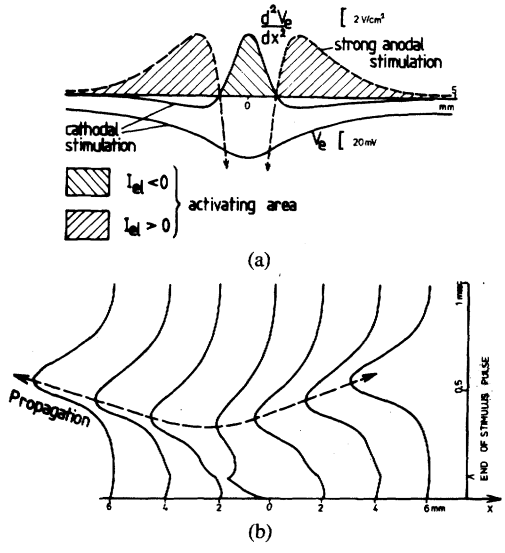


Fig. 4. (a) The lowest curve shows the extracellular potential $V_e$ generated at the axon by threshold current of $-290$ $\mu$A from a monopolar electrode at $z = 1$ mm. The activating function $d^2V_e/dx^2$ is plotted for $I_{el} = -290$ $\mu$A (full curve) and for strong anodal stimulation $I_{el} = 1450$ $\mu$A (broken curve). In the first case the positive (activating) part is in the cross hatched region in the middle, in the second case in the outer regions. (b) Action potential propagation. Horizontal axis distance along axon in millimeters, vertical scale time in milliseconds. Action potentials propagate with speeds $\pm 30$ m/s. They are produced by a rectangular current impulse of 0.1 ms duration and $I_{el} = -300$ $\mu$A is just above threshold. $\rho_e = 0.3$ k$\Omega \cdot$ cm.

4(a) and (16)] excitation with $I_{el} < 0$ is possible only within a short zone of the axon approximately equal to the distance $z$ of the electrode. For positive $I_{el}$ the ordinate axis of Fig. 4(a) must be inverted. Strong positive $I_{el}$ (with $I_{el}^{+} > 5 \cdot |I_{el,th}^{-}|$) produces two symmetrical action potentials at distances $x$ and $-x$ with $x$ roughly equal to $2z$. These action potentials propagate in both cases in the negative and positive $x$ direction as seen in Fig. 4(b) for $I_{el} = -300$ $\mu$A.

## The Myelinated Axon

Equations (1)–(3) are also appropriate for the myelinated axon. The membrane is active only at the nodes of Ranvier [Fig. 1(c)]. The length of the unmyelinated part can be chosen somewhat longer to correct for the imperfect insulation of the myelin sheet [11]. The corrected length $L$ of one active segment enters the computation. The analog of (4) for myelinated fibers is

$$\frac{dV_n}{dt} = \frac{1}{C_m} \cdot \left\{ \frac{1}{r_s \Delta x} (V_{n-1} - 2V_n + V_{n+1} + V_{e,n-1} - 2V_{e,n} + V_{e,n+1}) - \pi dL(i_{Na} + i_K + i_L + i_P)_n \right\}. \quad (4a)$$

Frankenhaeuser and Huxley had found that in the case of myelinated fibers, the HH equations have to be corrected by introducing a further sodium current $i_P$ [7]. Thus, (4a) must be completed by four FH differential equations for each node [4], [7]. Setting

$$C_m = \pi dLc_m \quad (5a)$$

leads (4a) to the analog of (6)

$$\frac{dV_n}{dt} = \frac{1}{c_m} \cdot \left\{ \frac{1}{r_s \pi dL \Delta x} (V_{n-1} - 2V_n + V_{n+1} + V_{e,n-1} - 2V_{e,n} + V_{e,n+1}) - (i_{Na} + i_K + i_L + i_P)_n \right\} \quad (6a)$$

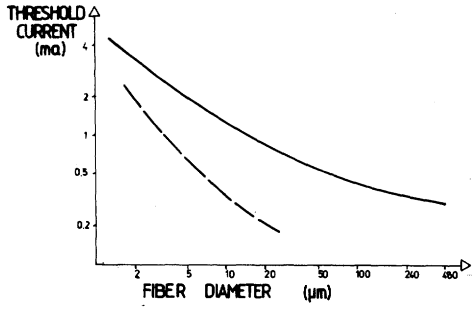


Fig. 5. Threshold current of monopolar electrode as a function of diameter $d$ of the axon. The electrode is situated 1 mm from an unmyelinated axon (full curve) and a myelinated axon (broken curve). Stimulation results from a rectangular cathodal impulse of 0.1 ms. Physical parameters are taken from squid nerve [5] resp. from *xenopus laevis* [7] for $\rho_e = 0.3$ k$\Omega \cdot$ cm in both cases. Length of simulated axon is 9 mm.

which is the tool to study the influence of parameters of fibers and electrodes on the electrical behavior of the myelinated axon.

From (6a) it is seen that the activating function for myelinated axons is given by the second difference quotient of the external potential along the axon in contrast to the second differential quotient for unmyelinated fibers. This fact results in different behavior only when small distances $z$ (less than the internodal length of about 1 mm) are used. Another difference between (6) and (6a) is the weighting of the activating function, but qualitatively, the myelinated and the unmyelinated case can be treated in the same way.

## Discussion

For a given geometry of the extracellular medium, the active regions of the axons are determined by purely geometrical considerations which can be extended to inhomogeneous external media. A method based on differential equations discretized in the coordinate along the axon may be used for the computations of threshold and superthreshold behavior of myelinated and unmyelinated axons. To find an estimation of the truncation error we half the grid until the solution is stable. The discretization length $\Delta x$ in the case of myelinated fibers is given by the internodal distance. To simulate an infinite axon, a length has to be considered where constant velocity of AP is reached for superthreshold stimulation.

An axon changes the extracellular potential also by its own activity, but only below 1 mV, whereas the intracellular contribution of voltage is high [1]. As the threshold for extracellular stimulation is about 30 mV, the influence of the axon to the extracellular potential is not essential and is not considered here but we find more accurate models in the literature [2], [3].

Our model allows us to study the influence of parameters to reach threshold, e.g., the dependence of the current of a monopolar electrode needed for excitation on its distance from an axon or the influence of fiber diameter on threshold current (Fig. 5). If it is possible to find the activating function $d^2V_e/dx^2$, we can use the model also for multichannel electrode stimulation and inhomogeneous media. The ionic currents can be stimulated by the two dimensional Fitzhugh model [12], the HH or FH equations, or any other submodel. Results of the analysis of external stimulation by different types of electrodes will be published in a forthcoming paper. Our results are in accordance with experiments, e.g., [13].

## References

[1] R. Plonsey, "The active fiber in a volume conductor," *IEEE Trans. Biomed. Eng.*, vol. BME-21, pp. 371–381, 1974.

[2] J. K. Woosley, B. J. Roth, and J. P. Wikswo, Jr, "The magnetic field of a single axon: A volume conductor model," *Math. Biosci.*, vol. 76, pp. 1–36, 1985.

[3] M. S. Spach and J. M. Kootsey, "Relating the sodium current and conductance to the shape of transmembrane and extracellular potentials by simulation: Effects of propagation boundaries," *IEEE Trans. Biomed. Eng.*, vol. BME-32, pp. 743–755, 1985.

[4] D. R. McNeal, "Analysis of a model for excitation of myelinated nerve," *IEEE Trans. Biomed. Eng.*, vol. BME-23, pp. 329-337, 1976.
[5] A. L. Hodgkin and A. F. Huxley, "A quantitative description of membrane current and its application to conduction and excitation in nerve," *J. Physiol. (London)*, vol. 117, pp. 500-544, 1952.
[6] J. J. Jack, D. Noble, and R. W. Tsien, *Electric Current Flow in Excitable Cells*. Oxford, England: Clarendon, 1975.
[7] B. Frankenhaeuser and A. F. Huxley, "The action potential in the myelinated nerve fiber of Xenopus Laevis as computed on the basis of voltage clamp data," *J. Physiol. (London)*, vol. 171, pp. 302-315, 1964.
[8] A. C. Scott, *Neurophysics*. New York: Wiley Interscience, 1977.
[9] H. Cohen, "Mathematical developments in the Hodgkin-Huxley theory and its approximations," *Lect. Math. Life Sci.*, vol. 8, pp. 89-124, 1976.
[10] H. Meves, "Hodgkin-Huxley: Thirty years after," *Current Top. Membranes Transport*, vol. 22, pp. 279-327, 1984.
[11] F. T. Dun, "The length and diameter of the node of Ranvier," *IEEE Trans. Biomed. Eng.*, vol. BME-17, 1970.
[12] R. Fitzhugh, "Impulses and physiological states in theoretical models of nerve membrane," *Biophys. J.*, vol. 1, pp. 445-466, 1961.
[13] J. B. Ranck, Jr, "Which elements are excited in electrical stimulation of mammalian central nervous system: A review," *Brain Res.*, vol. 98, pp. 417-440, 1975.

# Communication by Eye Closure—A Microcomputer-Based System for the Disabled

K. T. V. GRATTAN, A. W. PALMER, AND S. R. SORRELL

*Abstract*—**In this paper the development of hardware and software for an optical communication system based on the monitoring of deliberate eye blinks is shown for use by people with very severe disabilities. The system relies upon the use of software written for a simple home computer to interpret the eye blinks and construct messages, with the efficient use of the blink signal to access letters of the alphabet and a library of words.**

## I. Introduction and Background

Verbal communication is probably the most significant link between an individual and his or her human surroundings. A person deprived of this ability is severely handicapped in any relationship with society. The functional impairment of speech is usually, but not always, of nervous origin. Very frequently this is accompanied by impairments to other parts of the motor system. In the most severe cases, the disability is so great as to leave only the eyes as a potential means of communication. Since the individual is often literate and mentally active, it is important that efficient communication aids be developed to help alleviate his isolation. The motivation for the development of a communication aid came from contact with an organization which seeks to put disabled peoples' problems to engineers, and thus the exploitation of the recent developments in technology to aid the physically handicapped presents a challenge for the scientist and engineer. A number of companies worldwide manufacture nonvocal communication devices ranging in sophistication and cost, and catalogues of these aids are available [1]. A review of a number of such devices has been published by Rosen and Goodenough-Trepagnier [2] and comparisons of their cost and effectiveness were made. One major difficulty which remains with all these devices is the rate at which information is conveyed. In most aids this rate is up to ~100 times less than the rate of normal speech, thereby hindering direct "conversation" with an able-bodied person.

The use of switch closure by the disabled person opens up the possibility of a means of communication. In previous work [1] a number of switching systems have been proposed including the use of positive and negative breath pressure via a tube to the mouth, low contact pressure switches using the tongue and lips, in addition to noncontact switches such as acoustic devices responding to a particular pitch and optical devices. For patients with greater head mobility, the use of a head mounted wand or mouth stick has proved effective. In this work, the use of the recently developed fiber optic technology is represented in the discussion of a disabled persons' aid which is simple. While a switch with a proportional output—an output depending on a switch position—offers the possibility of greater information transfer than a simple two-level switch, the monitoring of a basic two-level natural process like the blink response is readily done by noncontact optical means. Gaze angle detection has been used in more sophisticated systems using modern imaging principles in various American universities [2] in proportional devices. It was considered that the use of a simple two-level blink principle, together with the now inexpensive optical fibers, sources and detectors, and a cheap home computer could lead to the development of a device which could be made widely available—in particular in a country where only very limited funds for these devices are accessible, mostly arising from small charitable organizations. In this case a communication aid was required which could utilize a patient's voluntary eye blinks to enable the individual to "write" a message on a VDU screen from preselected words, letters, or numbers. The general considerations were that the device must be simple to learn to use and operate, make efficient use of input signals to maximize the speed of communication, and be flexible to allow tailoring to individual needs.

Previous work on hardware development in this laboratory [3] had demonstrated that a simple binary code could be transmitted through the use of the eye blink response, but an increased degree of reliability in the production and sophistication of the content of the message produced was required. The approach of the work to be described was to refine the electronic hardware, keeping the complexity of this part to a minimum and using software routines on a microcomputer for the information processing and message construction.

## II. Text Composition—Design Considerations

Three modes of operation in a disabled aid may be used—direct selection, encoding, and scanning [4]. The first is inapplicable to the blink detection scheme herein, requiring for example, a method of "pointing" at the object of the selection. Encoding and scanning have been inconsistently categorized in the past as pointed out by Damper [5] in reference to the work of Heckathorne *et al.* [6]. In scanning the *timing* of an input is important as the control part of the aid will move the focus of the device to the next item without action by the user, the so called "autoscan" mode. Encoding is a way of reducing the set of input actions to allow for limitations in the user or device, e.g., Morse code. The timing of the inputs is not important and for a knowledgeable user even the display may be redundant, if error correction is available, again as exemplified by a skilled Morse code operator. When time (in the form of pulse duration) is a selection alternative, the distinction between the scanning and encoding processes is somewhat confused. In spite of the reservations by the authors on the desirability of teaching the user Morse code, this familiar code has been employed successfully in the work of Wilson [7] using a Morse code translation

Manuscript received June 24, 1985; revised April 21, 1986. This work was supported by REMAP.

The authors are with the Measurement and Instrumentation Centre, School of Electrical Engineering and Applied Physics, The City University, London EC1V 0HB, England.

IEEE Log Number 8609983.